

# Determining the Effects of Vapor Sorption in Polymers Using the Quartz Crystal Microbalance/Heat Conduction Calorimeter

Allan L. Smith<sup>\*</sup>, Sr. Rose B. Mulligan<sup>\*\*</sup>, and Hamid M. Shirazi<sup>\*\*\*</sup>

Chemistry Department, Drexel University, Philadelphia, PA 19104, USA

**Abstract:** The Quartz Crystal Microbalance/Heat Conduction Calorimeter (QCM/HCC) is a versatile instrument coupling both gravimetric and calorimetric techniques. The QCM/HCC is utilized to probe vapor sorption in thin films. Three parameters are measured simultaneously as a thin film undergoes vapor sorption namely: mass changes in the film ( $\pm 10\text{ng}$ ), corresponding thermal effects upon vapor sorption ( $\pm 100\text{nW}$ ), and motional resistance ( $\pm 0.5\Omega$ ) changes within the film. A range of film thicknesses ( $0.75\ \mu\text{m}$  to  $8.5\ \mu\text{m}$ ) of the polymer, Tecoflex<sup>®</sup> are cast on QCM's and the interaction of each film with ethanol and water is determined. From the direct calorimetric measurements, sorption enthalpies ( $\Delta_{\text{sorption}}H$  kJ/mol) are determined for the film-vapor interactions. Sorption isotherms are then analyzed for each film. The isotherms shown here generally display a linear Henry's Law dissolution relationship between the vapor pressure and the amount of vapor sorbed into the film. Motional resistance data provides a window to view viscoelastic effects of the polymer films upon vapor sorption. Motional resistance data are compared for ethanol sorption in a relatively thin ( $0.75\ \mu\text{m}$ ) and thicker ( $8.5\ \mu\text{m}$ ) Tecoflex<sup>®</sup> film.

**Keywords:** quartz crystal microbalances (QCMs), calorimetry, thin films, sensors, isotherm

---

\* present address: Masscal Corporation, W. Chatham, MA 02669

\*\* present address: Immaculata University, Immaculata, PA 19345

\*\*\* present address: Vecia, Inc., Ink Jet Division, New Castle, DE 19720

## Introduction

The interaction of polymer thin-films with solvent vapors has attracted much attention due to the broad range of applications in areas such as: the drying of polymer and paint coatings,<sup>1,2,3</sup> microlithography,<sup>4</sup> biological sensors,<sup>5-7</sup> polyimide protective coatings for microelectronic packaging,<sup>8</sup> flexible hosing and seals<sup>9</sup> and chemically sensitive, selective polymer coatings for organic vapor determination.<sup>10-14</sup>

Inherent in studying polymer-solvent applications is the necessity of exploring the complex changes in polymer film properties as the film undergoes vapor sorption. Upon vapor sorption not only does a polymer film gain mass, but structural changes within the film also occur, such as relaxational effects of the polymer side chains, free volume variations, glass transition temperature lowering and an increase in viscoelastic behavior. An added complexity arises because polymer sorption and swelling are specific for each polymer and dependent on the processing conditions.<sup>15</sup>

The Quartz Crystal Microbalance/Heat Conduction Calorimeter (QCM/HCC) is a relatively new gravimetric/calorimetric instrument used to probe the thermodynamic and rheological effects of thin film (typically 0.5 – 10  $\mu\text{m}$ )-vapor interactions.<sup>16</sup> An attractive aspect of the QCM/HCC is that it is an instrument capable of real-time sorption experiments while simultaneously measuring the thin film thermodynamic and rheological changes. Many current methods to determine rheological properties of polymers are not amenable to studying thin films. Data for thin films are often extrapolated from bulk samples, but errors often result because the substrate and deposition techniques differ for bulk samples versus films thus influencing the polymer structure and dynamics.<sup>17-19</sup>

Using the QCM/HCC, thin films are studied under isothermal conditions while the vapor activity in contact with the film is changed incrementally. Both sorption and desorption are monitored repeatedly over a wide range of vapor activities (typically between 0 and 0.90). Applications of the QCM/HCC studied so far include the hydration of pharmaceutical coatings,<sup>20</sup> alkylthiol monolayer formation on gold (ref. in press), hydrogen sorption of a palladium film,<sup>21</sup> protein hydration studies,<sup>22</sup> solvate formation of C<sub>60</sub>-piperazine thin films,<sup>23</sup> and interactions of various solvents with polymer films.<sup>16</sup>

The QCM/HCC combines the sensitive mass detecting capabilities of quartz crystal resonators with the heat detecting capabilities of thermopiles. Using the QCM/HCC, three aspects of polymer sorption are probed simultaneously: (1) mass changes upon sorption ( $\pm 10$  ng), (2) corresponding thermal effects ( $\pm 100$  nW), and (3) motional resistance changes in the polymer thin film ( $\pm 0.5 \Omega$ ). In this paper, we present experimental data on films of an aliphatic polyurethane polymer used for *in vivo* medical devices, with a trade name Tecoflex<sup>®</sup>. We used a variety of polymer film thicknesses (1) to explore the effect of film thickness on the sorption processes, (2) to evaluate the results in terms of sorption enthalpies and sorption isotherms, and (3) to monitor the QCM motional resistance changes upon sorption.

### **Quartz Crystal Microbalances**

A flat quartz disc with electrodes on both surfaces can be forced to oscillate in a transverse acoustic mode (motion parallel to the surface) by an RF voltage applied at the acoustical resonance frequency of the plate. This device is called a *transverse shear mode (TSM) quartz plate resonator*. A TSM resonator whose frequency is continuously monitored when a sample is deposited on its surface is known as a quartz crystal

microbalance (QCM). The frequency of the fundamental mode is inversely proportional to plate thickness. The development and applications of quartz plate resonators constitutes a venerable field in electrical engineering, dating back to World War II. Quartz plate resonators are the basis of accurate measurements of time, from quartz wrist watches to ultrastable frequency counters.

QCM's operate under the principle that the electrical properties of the quartz resonator are related to the mechanical properties of both the QCM and the film adhered to its surface. An oscillating QCM can be described using an equivalent circuit consisting of a series RLC resonant circuit in parallel with a shunt capacitance. These resonators have been used as sensitive microbalances for thin adherent films since the late 1950's, following the pioneering work of Sauerbrey.<sup>24</sup> Following the notation of Buttry and Ward,<sup>25</sup> the resonant frequency,  $f_0$ , of a quartz TSM resonator of thickness  $h_q$  is

$$f_0 = (\mu_q/\rho_q)^{1/2}/2h_q \quad [1]$$

where  $\mu_q$  and  $\rho_q$  are the shear modulus and density of quartz. The shift in frequency due to deposition of a film of the same acoustic impedance as quartz is proportional to the deposited mass per unit area of the film,  $\Delta m/A$ :

$$\Delta f = -\{2f_0^2 /(\mu_q\rho_q)^{1/2}\}\Delta m/A = -C \Delta m/A \quad [2]$$

where the mass per unit area,  $\Delta m/A$ , is linked to the product of the film thickness,  $h_f$ , and film density,  $\rho_f$ .

$$\Delta m/A = h_f \rho_f \quad [3]$$

For a 5 MHz crystal,  $h_q = 0.331 \text{ mm}$ ,  $C = 56.6 \text{ Hz}/(\mu\text{g}/\text{cm}^2)$  and the exposed surface area in the QCM/HCC is  $1.979 \text{ cm}^2$ . Lu and Czanderna<sup>26</sup> have reviewed the use of QCM's as film thickness monitors in vacuum deposition of metals and inorganic solids, an important industrial use since the 1970's. QCM's are useful because of their sub-nanogram sensitivity.

The electrical characteristics of an uncoated quartz QCM are well represented as a simple RLC damped resonator equivalent circuit with a complex impedance  $\mathbf{Z}_q$ . Using an impedance analyzer, it is possible to measure both the real and imaginary parts of  $\mathbf{Z}_q$  for TSW resonators.<sup>27-34</sup> The width of the resonance for an uncoated resonator is only 10-20 Hz, and the mechanical damping within the quartz that gives rise to this broadening can be determined by measuring the *motional resistance*,  $R$ , of the resonator (*vide infra*), typically  $\sim 10$  ohms. When thin, stiff films are deposited on the QCM surface the increase in  $R$  is small, but softer, thicker films (i.e., rubbery polymers 5-10 microns thick) can strongly increase  $R$ . Lee, Hinsberg, and Kanazawa<sup>29</sup> have measured the viscoelastic properties of polymer films using a phase locked oscillator circuit.

The impedance of a TSM resonator damped by a finite viscoelastic film can be described as the sum of two complex impedances.<sup>31,35</sup>

$$\mathbf{Z} = \mathbf{Z}_q + \mathbf{Z}_L \quad [4]$$

where the acoustic load impedance due to the film  $\mathbf{Z}_L$  contains both an inductive and a resistive part.<sup>31,36</sup>  $\mathbf{Z}_L$  is a function of four film parameters: shear storage modulus  $G_f'$ ,

shear loss modulus  $G_f''$ , thickness  $h_f$ , and density  $\rho_f$ . The shear moduli are functions of the frequency at which they are measured.<sup>37,38</sup> Lucklum and Hauptmann<sup>30</sup> and Janshoff, Galla, and Steinem<sup>39</sup> have reviewed the determination of shear storage modulus  $G_f'$  and shear loss modulus  $G_f''$  of thin viscoelastic films with TSM resonators. Even though the basic physics of damped TSW resonators is well understood, the effort to determine  $G_f'$  and  $G_f''$  from measurements of frequency shift and motional resistance change has been fraught with problems.<sup>40</sup> For very thin, rigid films, the frequency shift contains no information on either  $G_f'$  or  $G_f''$  because the Sauerbrey limit (Eq. 1) is reached. For thicker and/or lossier films the frequency shift and motional resistance depend on  $G_f'$  and  $G_f''$  in a complex manner not obvious by examining the equations. Our approach to determining  $G_f'$  and  $G_f''$  is presented in another reference.<sup>41</sup>

Because quartz resonators are not widely used to determine the mass of adherent polymer films, some historical perspective on the Sauerbrey equation and its limitations is warranted here. A 40-page review of the physics of coated piezoelectric oscillators and their electrical properties can be found in Chapter 2 of the Ph.D. thesis of H.M. Shirazi<sup>21</sup>, and these comments are based on that review. The work of Miller and Bolef<sup>42,43</sup> in 1968 constituted the first basis for the treatment of an oscillating quartz/film as a composite resonator. Lu and Lewis<sup>44</sup> extended this treatment to arrive at an extension of the Sauerbrey equation, subsequently termed the Z-match relationship. This method became widely used in the vacuum coatings industry because it provided a way to calculate mass change for coatings up to 50% of the thickness of the quartz resonator itself, but it required knowledge of the shear storage modulus of the coating as well as of the quartz. There is extensive experimental data in the literature validating the useable mass range of

the Z-match method for large mass loadings of rigid materials such as metallic films. But it was not until the more recent theories of coated oscillators that it became clear that the Sauerbrey equation is exact in the limit of zero coating thickness, independent of the modulus of the coating. It is also possible using power series expansion to calculate a first-order correction to the Sauerbrey equation for thin films<sup>41</sup>. The result is

$$\frac{\Delta f}{f_0} = \frac{\rho_f h_f}{\rho_q h_q} \left\{ 1 + \frac{4 h_f^2 \pi f_0^2 \rho_f J'}{3} \right\} \quad [5]$$

where  $h_f$  and  $h_q$  are the thickness of film and quartz oscillator,  $\rho_f$  and  $\rho_q$  are the densities of film and quartz, and  $J'$  is the shear storage compliance of the coating,

$$J' = \frac{G'}{(G'^2 + G''^2)} \quad [6]$$

measured at the oscillator frequency  $f_0$ . From the time-temperature superposition theory of viscoelastic properties, and from rheological data from dynamic mechanical analysis (DMA) taken at lower frequencies treated in the WLF formalism, it can be shown<sup>41</sup> that almost all polymers are viscoelastically stiff when their moduli are measured at 5 MHz, and that  $G' \gg G''$  and thus  $J' \approx 1/G'$ . For a typical value of  $G' = 10^9$  Pa, a 10  $\mu\text{m}$  film of density 1  $\text{g/cm}^3$ , the correction term in Eq. [6] is 1%. It is also clear from the data on the change of storage and loss modulus of a polymer when it absorbs a small plasticizer molecule that  $J'$  is virtually unaffected. These conclusions will not be modified if the operating frequency of the QCM differs substantially from 5 MHz (say, at one of its overtones), because  $G'$  is unaffected.

## Heat Sensors – Thermopiles

The QCM/HCC utilizes thermopiles as heat sensors to detect thermal gradients upon vapor sorption. A thermopile is one heat-sensing unit made from the combination of several semiconductor thermocouple plates, also known as Peltier plates. In the QCM/HCC, the thermopiles are in direct thermal contact with the brass electrodes which hold the QCMs. Thermal effects, due to vapor sorption by a thin film, travel through the thermopiles to the underlying heat sink.

When at steady state, the heat flow from the sorption event is directly proportional to the thermopile potential,  $U$ . The thermal power is:<sup>45</sup>

$$P = \varepsilon U \quad [5]$$

where  $\varepsilon$ , is the calibration constant (W/v) for the thermopiles. The rate of heat absorbed or released,  $P$ , is related to the heat quantity,  $dQ$ , during a time  $dt$ :

$$dQ = \varepsilon U dt \quad [6]$$

leading to the relationship of heat flow,  $dQ/dt$  and thermopile potential,  $U$ :

$$P = dQ/dt = \varepsilon U \quad [7]$$

If the sorption process is not steady state such as the case of a fast reaction, this process is characterized by the Tian equation:<sup>46</sup>

$$P = \varepsilon(U + \tau(dU/dt)) \quad [8]$$

where  $\tau$  is the time constant of the calorimeter.

### Enthalpy of Sorption

As vapor molecules from the gas phase are sorbed into an absorbent film, the QCM/HCC measures both the mass and corresponding thermal signals. The vapor activity in contact with the film is incrementally changed and held constant for a period of time.

Equilibrium is attained when the vapor is sorbed and desorbed at the same rate in the film. In the QCM/HCC measurements, this is visible when the mass and thermal traces level off (typically  $\pm 0.2$  Hz and  $\pm 0.3 \mu\text{W}$  respectively) after the vapor concentration has been changed. The experiments were performed under isothermal conditions ( $25^\circ\text{C}$ ) and the amount of sorbed vapor was dependent on the controlled vapor pressure in contact with the thin film.

To determine the enthalpy of sorption, integration of the measured heat quantity yields:

$$Q = \varepsilon \int_1^2 U dt \quad [9]$$

where  $Q$  is the integral heat of sorption. The integral calorimetric heat is thus:<sup>47</sup>

$$q_i = \frac{\varepsilon \int_1^2 U dt}{n} \quad [10]$$

where  $n$  are the moles of adsorbed gas and  $q_i$  is the molar enthalpy of sorption (kJ/mol).

## Sorption Isotherms

Sorption isotherms are often used to characterize solid-vapor interactions. Isotherms measure the amount of vapor absorbed by a given amount of absorbent,  $g_{\text{adsorbate}}/g_{\text{adsorbent}}$ , as a function of the vapor pressure. Many studies have explored the characterization of vapor sorption in polymeric materials.<sup>48,49,50,51</sup> Vapor sorption is likened to a diluent being added to a polymer. Depending on the diluent, an increase in this amount can noticeably decrease the polymer  $T_g$ . An example of this includes the hydration of polyamides. The  $T_g$  of several polyamides (Nylon 6, Nylon 6,6, Nylon 4,6) with no added water is  $\sim 67^\circ\text{C}$ . When water is added to a hydration level of  $0.10 g_{\text{water}}/g_{\text{polymer}}$ , the  $T_g$  is lowered to  $\sim -33^\circ\text{C}$ . This is an  $80 - 100^\circ\text{C}$  change in the  $T_g$  in a relatively small hydration range.<sup>52</sup>

The shape of the sorption isotherm reveals information as to whether the polymer is in the glassy or rubbery state. This depends on the type of polymer being studied and the type of vapor being used for the sorption. Vapor sorption in a polymer causes varying degrees of plasticization. The plasticizing effect is viewed when the polymer undergoes a glass transition. The lower vapor activity ranges of an isotherm are frequently described using the Dual-Mode Model. The model uses a combination of Henry's Law to explain sorption in the low solubility limit and a Langmuir sorption isotherm to describe the sorption in the excess free volume of the glassy state.<sup>50</sup>

At the higher vapor activities,  $\geq 0.7$ , the polymer vapor sorption is often characterized using the Flory-Huggins model.<sup>50</sup> This model describes the non-ideal behavior of sorption in a rubbery polymer having passed its glass transition temperature,  $T_g$ , and is noted as an upward concave curvature of the isotherm.<sup>49</sup>

From our QCM/HCC experiments, sorption isotherms are presented for both water and ethanol sorption in the Tecoflex films. Using the QCM/HCC, sorption of the polymer films was measured at a much higher frequency (e.g. 5 MHz versus 10 Hz) than several past studies presented in the literature.<sup>17,53,54</sup> The time scale used in measuring vapor sorption of a polymer influences the polymer  $T_g$ . When the probing frequency is 5 MHz, corresponding polymer relaxation times of the polymer backbone are not permitted. In this case, the polymer behaves as a rigid body and has a corresponding high shear storage modulus,  $G'$ .<sup>55</sup> For a much lower probing frequency (e.g. 10Hz), the polymer has time to reorient its chain segments and relieve any strains imposed by the stress. As the strained chains relax to lower energy conformations, there is a corresponding decrease in the shear storage modulus.<sup>55</sup> Because the QCM/HCC probes a polymer film at a high frequency, it is expected that the polymer  $T_g$  far exceeds its value determined by low frequency techniques (DSC, TGA). Thus, virtually all polymers free of solvent should be glassy when measured at 5 MHz.<sup>41</sup>

## **Experimental**

### **Instrumentation**

The QCM/HCC contains two 5MHz, AT cut, quartz crystal microbalances (Maxtek, Santa Fe Springs, CA, P/N 149211-1). One QCM is coated with the sample film while the other uncoated QCM is used as a reference. Each QCM is placed on two D-shaped brass electrodes. The electrodes serve in applying the RF voltage which causes the QCM to oscillate at its resonant frequency. Thermopiles (Melcor, Trenton, NJ, OTO.8-66-OF) are used to measure the heat flow from the sorption processes. The thermopiles are in direct, thermal contact with the two D-shaped brass electrodes upon which the sample

and reference QCM's are placed. The differential of the sample and reference thermal signals are fed to a DC low noise preamplifier (Nanovoltmeter, Model N15, EM Electronics, UK). A diagram of the QCM/HCC calorimetric chamber, designed, by Ingemar Wadsö of Lund University, in 1997, is shown in Figure 1.<sup>20</sup>

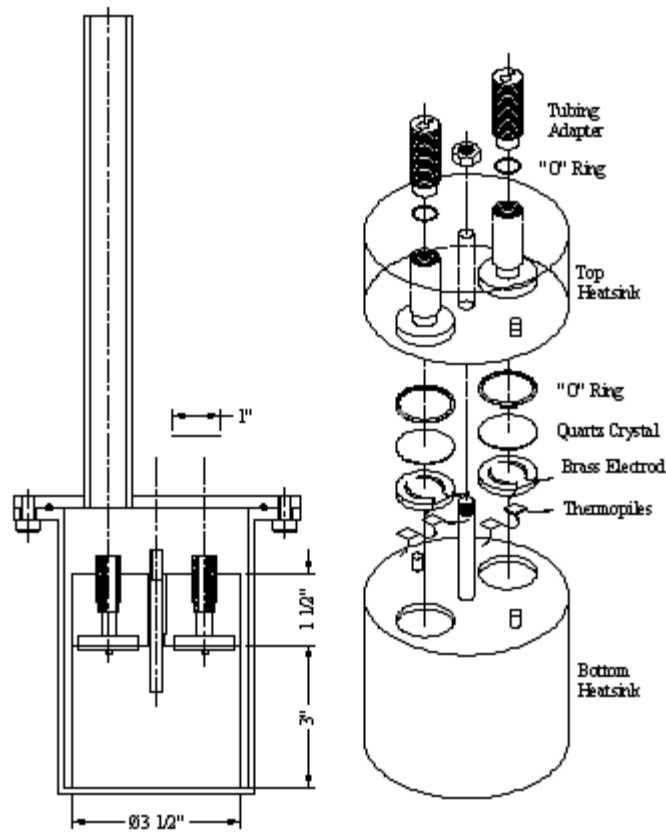


**Figure 1.** A schematic diagram of the QCM/HCC calorimetric chamber.<sup>20</sup>

The sample QCM is driven by a Maxtek, PLO-10, Phase Lock Oscillator which provides an RF voltage to maintain the QCM at its resonant frequency. The PLO-10

serves a two-fold purpose by providing a readout of the QCM frequency and a voltage output related to the motional resistance.

The gas flow is controlled by two mass flow controllers (Unit 8100). Nitrogen (BOC, grade 5.0) is generally used as the carrier gas. One mass flow controller sends the carrier gas to a glass gas bubbler. The vapor leaving the gas bubbler travels downstream to a mixing tee. At this point, carrier gas from the second mass flow controller is introduced. The desired vapor activity is controlled by mixing different compositions of the dry carrier gas with the saturated vapor leaving the gas bubbler. A relative humidity meter (RH-100, Sable Systems, NV) is used to confirm the water vapor activity reaching the QCM/HCC chamber.

The calorimetric chamber is sealed and placed in a constant temperature bath (Tronac 1250) with the temperature controlled to  $\pm 0.0001^\circ\text{C}$ .

### **Sample Preparation**

Tecoflex, HP-60D, is a cycloaliphatic, poly(ether urethane), synthesized and distributed through Thermedics Polymer Products (Woburn, MA). Tecoflex is commonly used in medical applications and has been explored as a possible gas vapor sensor.<sup>56</sup> The polymer has a reported density of  $1.11\text{ g/cm}^3$  and two glass transition regions with the soft portion  $T_g \sim -60^\circ\text{C}$  and the hard portion  $T_g \sim 40 - 50^\circ\text{C}$ . Tecoflex pellets were dried in an oven prior to dissolving in chloroform. Solutions of various concentrations (20 – 100 mg/ml) were prepared so as to vary the solution viscosities and create films of varying thicknesses.

Prior to coating, each QCM was cleaned in Piranha solution, (one part 30%  $\text{H}_2\text{O}_2$  in three parts 98%  $\text{H}_2\text{SO}_4$ ). Cleaning included: immersing each QCM in the Piranha

solution for ~ 2 min., rinsing vigorously with deionized water and drying with a stream of nitrogen gas. The QCM's were then stored in an oven for further drying.

Films were cast on one side of each QCM using one of two methods, spin coating or drop coating. For the spin coating, two procedures were used: (1) a single initial deposition of Tecoflex solution before spinning and (2) a continuous deposition of Tecoflex solution as the QCM was spinning. The 0.75 $\mu\text{m}$ , 0.83 $\mu\text{m}$  and 8.5  $\mu\text{m}$  films were coated with an initial deposition of ~ 2mL of Tecoflex solution placed on the center of the QCM. The spin coater was set at a range of 2000 – 3000 rpm for 45 – 60 sec. depending on the desired film thickness and solution viscosity. The 0.78 $\mu\text{m}$ , 1.1 $\mu\text{m}$ , and 2.09 $\mu\text{m}$  films were cast using a continuous deposition of Tecoflex solution. The 4.7  $\mu\text{m}$  film was the only one to be cast by drop-coating. The drop coating process involved dropping ~ 5mL of the Tecoflex solution via a glass pipet onto the QCM surface. The solution was allowed to spread naturally while the solvent evaporated. To anneal/dry the films, the polymer coated QCM's were placed in an oven at 50°C for at least 2 hours.

## **Experimental Methods**

The Tecoflex films were studied for their sorption of water vapor and ethanol vapor. Prior to each experiment, the polymer coated QCM's were placed in the QCM/HCC chamber and further dried with a steady stream of dry N<sub>2</sub> gas. Before and after the experiments, the thermopiles were electrically calibrated. Each experiment consisted of vapor activity changes in incremental steps (water 0.16 and ethanol typically 0.07). The polymer films were conditioned prior to the actual measurements. Conditioning included securing the coated QCM in the chamber and exposing the film to the second highest incremental vapor activity. The vapor activities were then decreased using the same

vapor activity increments and time scale used in the experiments. Input parameters on the LabView VI included the length of time for each sorption step and the incremental change in vapor activity. As sorption occurred, the corresponding mass, thermal and motional resistance changes were monitored. The process continued for five stepwise increasing steps of vapor activity and likewise for five decreasing steps. Two to four repeated cycles were recorded for each experiment. Table 1 and Table 2 display the parameters for the water and ethanol sorption experiments, respectively.

**Table 1.** Tecoflex - Water Sorption Experiments

File	Water Vapor Activity / $a_w$ $p/p^o$ 25°C	Incremental Step for $a_w$	Time for each step min.	Film mass $\mu\text{g}/\text{cm}^2$	Film thickness $\mu\text{m}$
02-01-08-2	0 - 0.80	0.16	26	83	0.75
01-08-07-1	0 - 0.80	0.16	18	93	0.83
99-10-26-2	0 - 0.80	0.16	26	119	1.1
01-11-20-2	0 - 0.80	0.16	26	523	4.7
01-09-11-1	0 - 0.80	0.16	70	946	8.5
01-09-27-1	0 - 0.80	0.16	70	946	8.5
01-12-20-3	0 - 0.80	0.16	70	946	8.5

**Table 2.** Tecoflex - Ethanol Sorption Experiments

File	EtOH Vapor Activity / $a_{\text{EtOH}}$ $p/p^0$	Incremental Step for $a_{\text{EtOH}}$	Time for each step min.	Film mass $\mu\text{g}/\text{cm}^2$	Film thickness $\mu\text{m}$
02-01-09-3	0 - 0.32	0.064	26	83	0.75
01-08-30-1	0.26 – 0.58	0.064	26	83	0.75
02-01-10-1	0.26 – 0.58	0.064	26	83	0.75
99-07-15-1	0.13 – 0.45	0.064	26	86	0.78
99-07-30-1	0.13 – 0.64	0.128	26	227	2.09
01-11-26-1	0.26 – 0.58	0.064	26	522	4.7
01-09-06-1	0.26 – 0.58	0.064	70	946	8.5
01-09-25-1	0.26 – 0.58	0.064	70	946	8.5

The mass per unit area of each film was determined using the Sauerbrey relationship, Eq. 2. For the Sauerbrey equation, the frequency of each uncoated QCM was compared with the QCM frequency after the solvent evaporated from the polymer film. The thickness of each film was found by utilizing the relationship between the polymer film mass and density.

## Results

### Water Sorption

Five different films were used to study the water sorption of the polymer Tecoflex with the hydration ranges spanning water vapor activities,  $a_w$ , of 0 to 0.80. Results of the sorption of the 8.5  $\mu\text{m}$  film are shown in Figure 2.

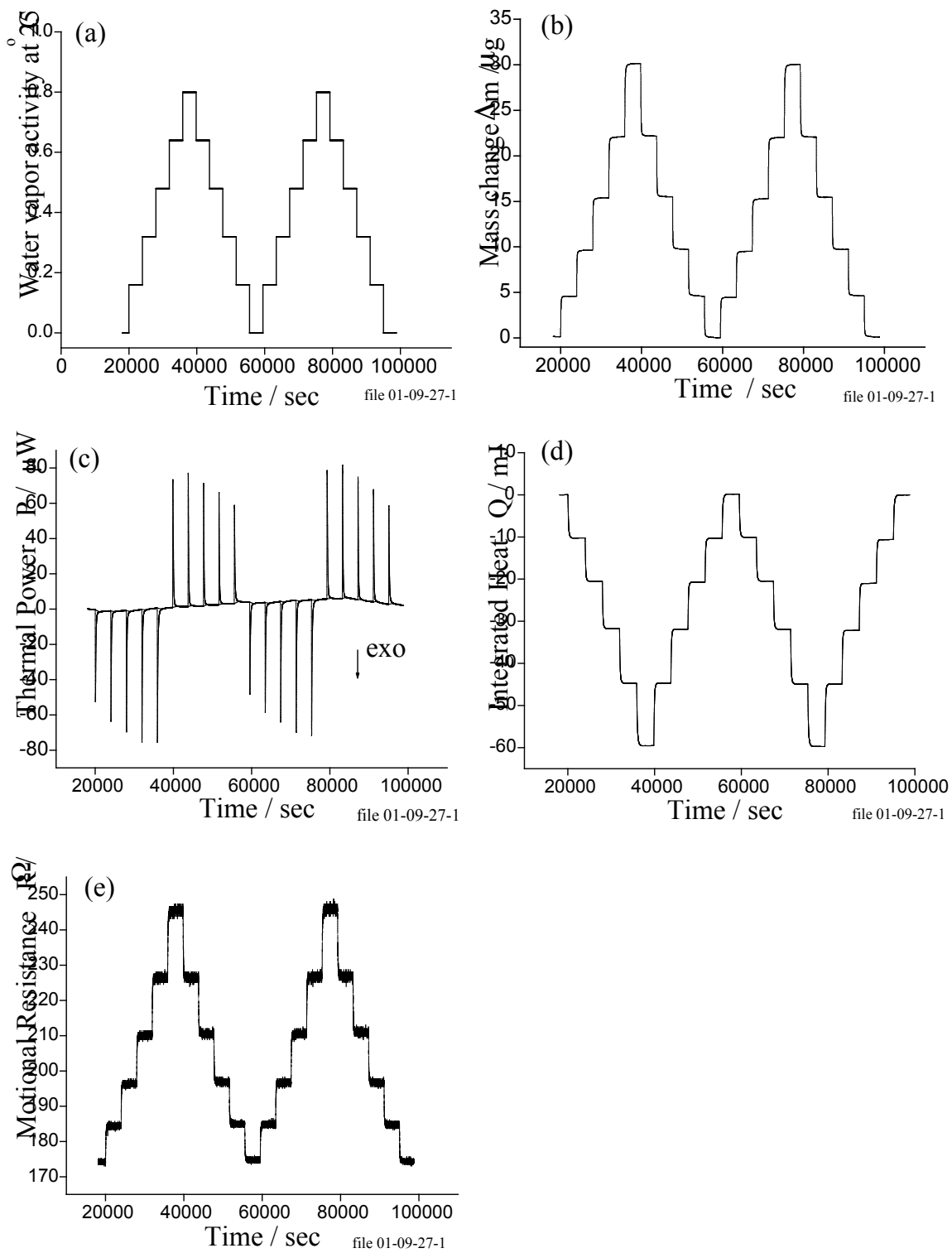


**Figure 2.** Tecoflex/water sorption, 8.5  $\mu\text{m}$  film, at 25°C. a) applied water vapor activity,  $a_w$ , b) mass trace, c) thermal power, d) integrated heat, e) motional resistance,  $R$

Several panels are shown in this figure. In graph (a) the incremental step-wise changes in the water vapor activity,  $a_w$ , are displayed. The polymer film was subject to two full cycles of sorption and desorption in this experiment. This graph is the applied water vapor activity as controlled by the mass flow controllers. As the water vapor interacted with the polymer film and was absorbed, corresponding mass changes were detected. These mass changes are recorded in (b). As can be seen in the graph, the mass uptake and release by the polymer film was repeatable with no noticeable hysteresis occurring. Graph (c) depicts the corresponding thermal changes due to sorption. As the film absorbed water, the downward, negative peaks represent exothermic events, while the upward, positive peaks are endothermic events. The integrated step-wise changes in the heat are shown in graph (d). The thermal peaks were integrated using the software Origin (Microcal Software, Northampton, MA). The difference in heat (mJ) was then determined for each sorption step. Graph (e) depicts the change in motional resistance,  $R$ , of the QCM resonator as the Tecoflex film underwent water sorption. The motional resistance provides a view of the energy loss within the system and measures the damping effect of the film cast on the QCM. The motional resistance of an uncoated QCM is typically 12  $\Omega$ .

### **Ethanol Sorption**

Tecoflex films varying in thickness from 0.75 to 8.5  $\mu\text{m}$  were exposed to ethanol vapor at 25°C and the sorption processes were monitored. Figure 3 displays the results for the 8.5  $\mu\text{m}$  film subject to ethanol vapor activities ranging between 0.26 – 0.58.

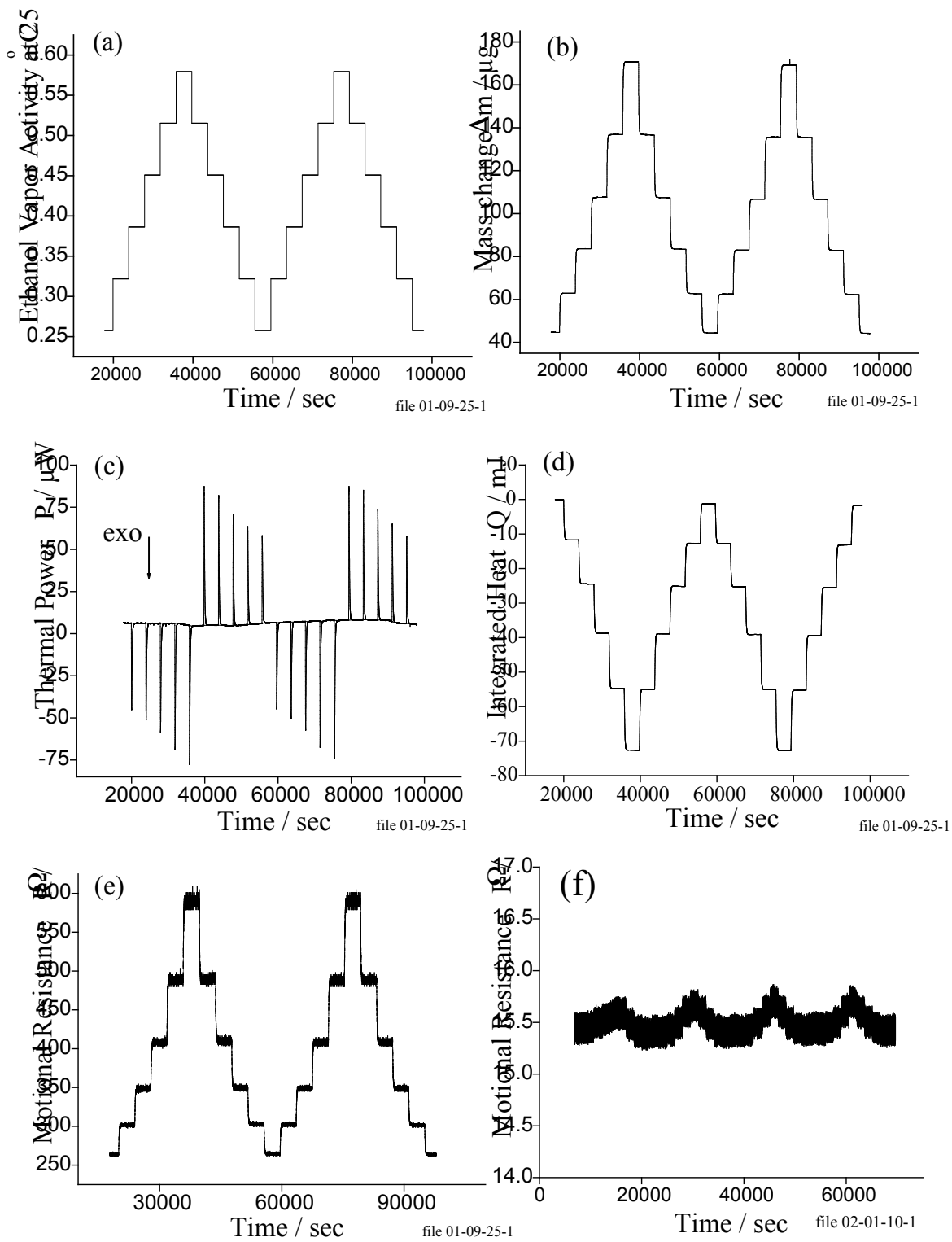


**Figure 3.** Tecoflex/ethanol sorption, 8.5  $\mu m$  film,  $a_{EtOH}$  range from 0.26 – 0.58, at 25°C. a) applied ethanol vapor activity, b) mass trace, c) thermal power, d) integrated heat, e) motional resistance,  $R$ , and f) motional resistance,  $R$ , of a 0.75  $\mu m$  film.

Graph (a) is a plot of the applied ethanol vapor activity interacting with the film at each stepwise change. The corresponding mass changes are shown in graph (b). The sorption processes over the two cycles were repeatable with no evidence of hysteresis. At the highest ethanol activity, it is noted that almost fifty percent more ethanol is sorbed than at the lower activities. This is consistent across all film thicknesses in these experiments. In (c), the thermal traces for the vapor sorption are shown. The sorption steps are the exothermic, negative directed peaks while the desorption steps are the endothermic, positive directed peaks. As equilibration was reached the thermal signals returned to a stable baseline. The integrated heat for each sorption step is plotted in (d). In (e) the motional resistance changes are depicted. As the film sorbed ethanol, the motional resistance increased indicating increased damping effects in the polymer film. The dry film had a motional resistance,  $R$ , of  $175 \Omega$ , which increased to  $\sim 263 \Omega$ , at an ethanol vapor activity of 0.26. At a vapor activity of 0.58,  $R$  increased to  $\sim 590 \Omega$ , approximately a 300% increase in the motional resistance of the dry film. Plot (f) depicts the motional resistance change in a  $0.75 \mu\text{m}$  film upon vapor sorption within the 0.26 – 0.58 activity range. A comparison of the motional resistance changes of the  $8.5 \mu\text{m}$  and  $0.75 \mu\text{m}$  films is discussed in the following sections.

## Discussion

### Enthalpy of Sorption

Figure 4 summarizes the results of water sorption in five different Tecoflex films. The steady-state mass and thermal traces indicate that equilibrium was reached upon both sorption and desorption. The  $\Delta_{\text{vaporization}}H$  of water at  $25^\circ\text{C}$  is  $+44 \text{ kJ/mol}$ .<sup>57</sup> The magnitude of the enthalpy values shown here cluster about  $44 \text{ kJ/mol}$ . The error bars

have been removed for clarity. For the sorption steps the average standard deviation was  $\pm 2$  kJ/mol across all film thicknesses while the desorption steps had a  $\pm 3$  kJ/mol standard deviation. The reversibility of the water-polymer interactions and the measured enthalpy values, lead to the conclusion that the intermolecular interaction among the water molecules in the liquid state are similar to the mean of the interaction between the water molecules and the various accessible functional groups on the Tecoflex polymer.

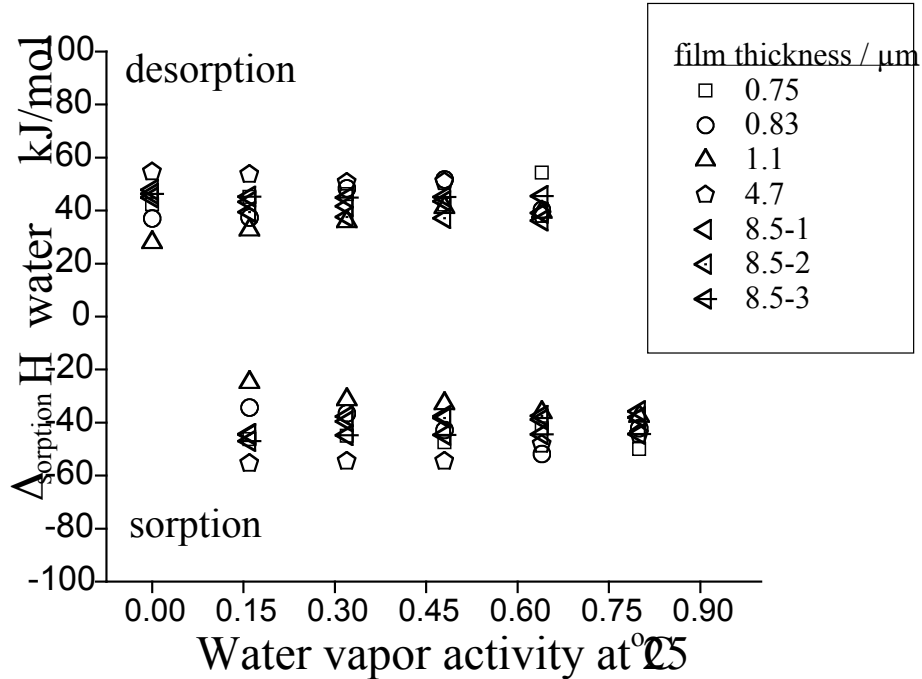


**Figure 4.** Enthalpy of water sorption in Tecoflex films as a function of film thickness and water vapor activity.

At the lower water vapor activities, a broader distribution among the enthalpy values is noted. The drop-coated 4.7 $\mu\text{m}$  film had enthalpy values higher in magnitude than 44 kJ/mol, while the 1.1  $\mu\text{m}$  film, spin-coated in the continuous manner (*vide supra*), enthalpy values are slightly lower in magnitude. At the higher water vapor activities ( $\geq 0.6$ ) the 4.7  $\mu\text{m}$  and 1.1 $\mu\text{m}$  films exhibit sorption enthalpies closer in value to the other films. The 8.5  $\mu\text{m}$  film was subject to three experimental runs. Two of the runs were performed within a two week span (8.5 $\mu\text{m}$ -1, 8.5 $\mu\text{m}$ -2). The third run was performed three months later (8.5 $\mu\text{m}$ -3). In the time period between the experiments, the film coated QCM was stored in a closed vessel at ambient conditions. For this particular polymer, the three month aging period did not show any prominent deviations from the two earlier measurements.

Figure 5 displays the  $\Delta_{\text{sorption}}H$  results for five different Tecoflex films undergoing ethanol sorption. The  $\Delta_{\text{vaporization}}H$  for ethanol at 25 $^{\circ}\text{C}$  is +42.3 kJ/mol. The values for the five different film thicknesses cluster about 40 kJ/mol. The measured enthalpy magnitude also suggests that the mean Tecoflex – ethanol intermolecular attractions are similar in to the liquid ethanol – ethanol interactions. Unlike the plot depicting the water sorption enthalpies, the ethanol sorption displays a broader distribution of values at the higher vapor activities. From the larger mass uptake of each film and the larger motional resistance changes recorded upon vapor sorption, ethanol is a more effective plasticizer of Tecoflex than is water.

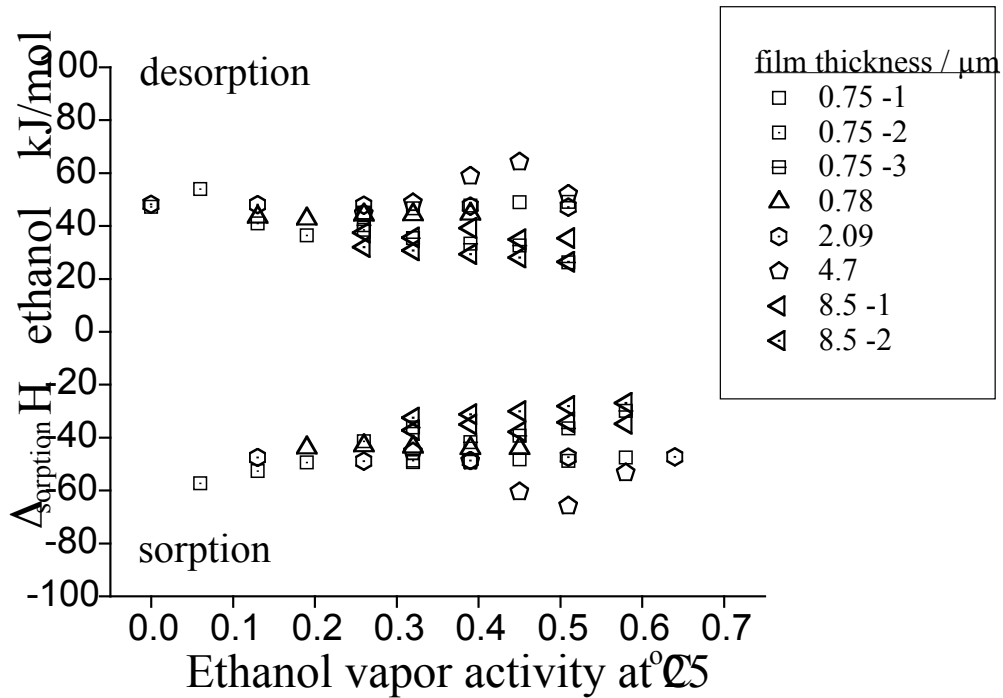


**Figure 5.** Enthalpy of ethanol sorption in Tecoflex films as a function of film thickness and ethanol vapor activity.

Upon both sorption and desorption, the enthalpy values of the 4.7  $\mu\text{m}$  film show a slight deviation at the higher vapor activities. For ethanol sorption in this particular polymer film, the drop-coating method of coating the film does appear to have an effect on the sorption. Researchers note that coating methods are known to have an effect on the chain interactions as a polymer film dries.<sup>58</sup> The measurements on this film were done prior to our capability of measuring the motional resistance,  $R$ , of the film upon vapor sorption. Further studies utilizing the measured  $R$  value will provide a window as to some of the rheological differences in the coating methods. This film was also studied using a home-built crystal oscillator. In driving the crystal oscillation, the home built oscillator generated excess heat in the QCM. This heat was detected by the thermopiles

and renders this set of enthalpy data as suspect. The results of this data set are shown here for the sake of presenting the QCM/HCC capabilities and modifications.

The two measurements of the 8.5  $\mu\text{m}$  film taken two weeks apart have a  $\pm 5$  kJ/mol deviation from each other. The two runs were completed using different QCM oscillator drivers. The first measurement on the 8.5  $\mu\text{m}$  film (8.5-1) was made using the home-built oscillator driver while the second measurement (8.5-2) on the 8.5  $\mu\text{m}$  film was measured using the Maxtek PLO. The PLO oscillator, like the home-built model, would generate an added heat in trying to drive the lossier film, however in this case a lower powered PLO was used. Using this, we had the capability of generating less power in the crystal, calculating the amount of excess heat generated, and accounting for this in the thermal signals. The second study of the 8.5  $\mu\text{m}$  film revealed motional resistance changes of  $\sim 400 \Omega$  over the span of the ethanol vapor activities. This is the largest motional resistance change of the studies shown here. The larger amount of ethanol sorbed in the film compared with water and the large motional resistance changes suggest that the film was becoming lossier than seen on previous films.

The direct sorption enthalpy measurements reveal a powerful capability of the QCM/HCC. Sorption enthalpies are traditionally measured using a Van't Hoff analysis of the sorption process over a range of temperatures. Because this process is time consuming, sorption enthalpies of polymer thin films are not frequently measured. Studies involving the hydration of the protein lysozyme were used to compare sorption enthalpy values measured with the QCM/HCC versus previously reported values obtained through a Van't Hoff analysis<sup>22</sup>. Our measurements using the QCM/HCC were in close agreement and showed the same sorption enthalpy trends as those measured by

several researchers including Bone<sup>59</sup> who utilized dielectric loss measurements at different temperatures, and Lüscher-Mattli<sup>60</sup> who gravimetrically measured water sorption at different temperatures.

### Sorption Isotherms

The sorption isotherms for the water and ethanol sorption measurements are shown in Figures 6 and 7. For both plots, the mass of the water and ethanol sorbed in the film is plotted versus the vapor activity.

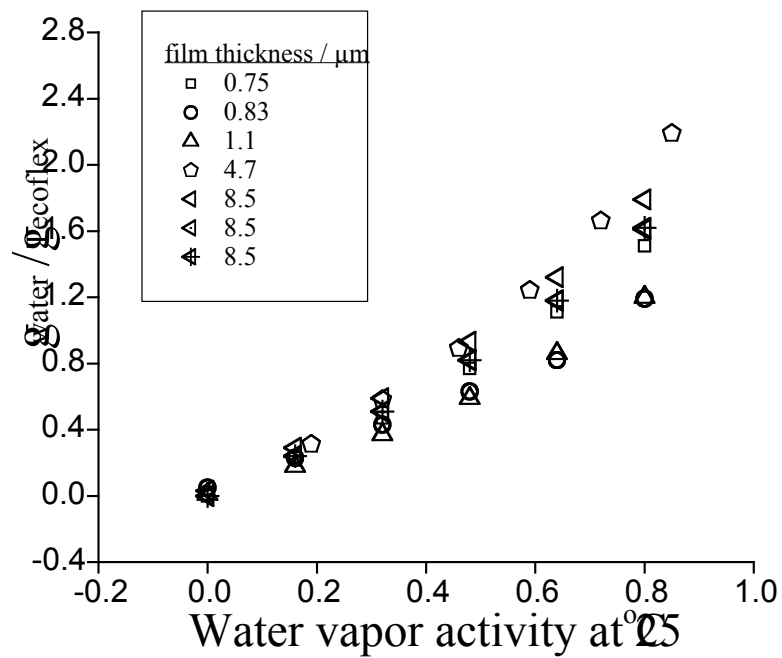


**Figure 6.** Water sorption isotherm of the polymer Tecoflex at 25°C. Varying film thicknesses are displayed in the legend.

The water sorption isotherm in Figure 6 shows continuity between the different film thicknesses and the amount of water being sorbed. In the low vapor activity ranges ( $\sim 0.5$ ), all films show a linear dependence of the amount of vapor sorbed versus the vapor

activity. The drop-coated 4.7  $\mu\text{m}$  film is the only film to show a significant concave curvature in the isotherm at the higher vapor activities ( $\geq 0.7$ ).

The ethanol sorption isotherm in Figure 7 contains a slightly broader distribution in the sorption values. The individual isotherms for each film undergoing ethanol sorption also display a linear behavior. When comparing mole ratios, approximately double the amount of ethanol was sorbed into the Tecoflex films compared to the water sorption. The 4.7  $\mu\text{m}$  drop-coated film behaved differently by sorbing almost 50% more ethanol than the other films.

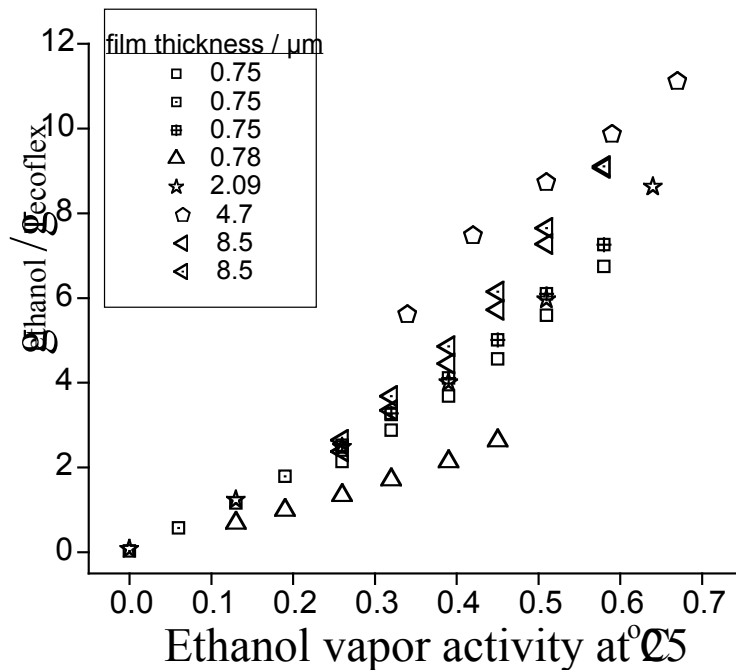


**Figure 7.** Ethanol sorption isotherm of the polymer Tecoflex at 25°C. The different film thicknesses are displayed in the legend.

The linear nature of the isotherms in the low activity range ( $< 0.35$ ) is indicative of Henry's Law solubilities where the solubility of the gas in the polymer is a function of

the vapor pressure. In this region, the dissolution of the gaseous adsorbate into the polymer is being measured. At higher vapor activity ranges (0.35 – 0.7) and/or higher pressures, the Langmuir portion of the Dual-Mode Model becomes influential.

Zhang *et.al.* utilized QCM's to study polymer film (0.35 to 0.55  $\mu\text{m}$  thick)  $\text{CO}_2$  vapor sorption as a function three parameters: pressure (0 to 19 atm), thermal conditioning of the films, and temperature.<sup>51</sup> The films in the study exhibit both the Henry's Law linear region (at pressures of 0 to  $\sim 1$  atm) as well as a Langmuir contribution ( $>1$  atm) attributed to hole-filling mechanisms in the film. Films subject to the two thermal conditioning methods displayed very similar trends in the shapes of the isotherms to the as-cast films not subject to the thermal conditioning. The as-cast film had a greater Langmuir sorption capacity at the higher pressures than the conditioned films. The general shape of each isotherm was preserved at each temperature although the amount of vapor sorption differed at each temperature. In their studies, the researchers make note of the difficulty in repeating sorption isotherm measurements. In their repeated experiments, sorption differences of up to 20% of the measured sorption were recorded.

As an added feature, Zhang, *et. al.*, used the Henry's Law solubility coefficients found from their isotherm fits, and plotted these values versus the inverse temperature to determine sorption enthalpies via the Van't Hoff relation.<sup>51</sup> With the QCM/HCC we are able to directly measure the enthalpy of sorption as shown above.

Russell and Weinkauff in their QCM's studies of the polymers, poly(methyl methacrylate) (PMMA) and poly(vinyl acetate) (PVAc), compared vapor sorption in films cast by two different methods: plasma polymerized films versus films cast from a polymer solution.<sup>50</sup> The studies were done under isothermal conditions ( $30^\circ\text{C}$ ) and 1 atm

pressure. Sorption isotherms for PMMA and the interaction with methanol, water, and acetone were plotted. For PMMA, the water and methanol sorption isotherms closely resemble those in this study. Acetone sorption isotherms had the added Flory-Huggins feature of a concave curvature at the higher vapor activities. For PVAc, sorption isotherms were plotted for water, hexane, and acetone. For the water, the Henry's Law portion of the isotherm dominated, while hexane and acetone both showed Langmuir contributions and the acetone sorption also revealed Flory-Huggins model characteristics.

QCM technology provides a valuable window into probing sorption isotherms of thin, polymer film samples. Comparisons are drawn here to highlight various factors which may affect the sorption isotherms, namely: the type of polymer used, the vapor adsorbate, casting methods of the film, the uniformity of the film thickness, and the temperature and pressure. While the results for ethanol absorption in the thickest (8.5 $\mu\text{m}$ ) film begin to exhibit differences from those of thinner films, it was not possible in these experiments to isolate the causes of these discrepancies.

### **Motional Resistance Changes**

Figure 3 (e) and (f) display a comparison between two films (8.5 $\mu\text{m}$  and 0.75  $\mu\text{m}$ ) undergoing ethanol vapor sorption. The ethanol sorption data are shown to display the plasticizing effects ethanol appeared to have in the polymer film. In part (f) of Figure 3, the data for the change in motional resistance of a 0.75  $\mu\text{m}$  film is plotted. The dry film has an initial motional resistance of 15.4  $\Omega$ , while the uncoated QCM had a R of  $\sim 12 \Omega$ . For the highest vapor activities, the maximum R of the film is 15.7  $\Omega$ . The small  $\Delta R$  changes reveal that the film is behaving as a rigid body adhered to the QCM surface over the range of vapor activities. In contrast to this is part (e) which depicts the 8.5  $\mu\text{m}$  film.

The dry film in this case has an initial motional resistance of  $175 \Omega$  which reflects a one order of magnitude increase over an uncoated QCM. A stepwise motional resistance change is readily seen corresponding to each change in the vapor activity. As the polymer film sorbs more of the vapor, the increased motional resistance indicates a slight increase in the viscoelasticity of the film. Because the QCM measurements are taken at a relatively high frequency, (e.g. 5MHz), the  $T_g$  of the polymer is increased. Therefore, although the polymer is undergoing vapor sorption, the film remains in a rigid state compared to polymer sorption at much lower frequencies.

A polymer film in its glassy state has a high shear storage modulus,  $G_f'$  ( $\sim 1\text{GPa}$ ) and low shear loss modulus,  $G_f''$ . In this case the film resonates synchronously with the QCM and the QCM acts in its gravimetric regime, that is, as a microbalance. As a polymer film swells, its viscoelastic properties influence its behavior and the upper film surface lags in its oscillation when compared to the QCM /film interface. In this case, the  $G_f'$  can often decrease to 1 MPa indicating that the material has become softer and more lossy.<sup>61</sup> The motional resistance changes,  $\Delta R$ , reflect energy dissipation in the film. Although the  $\Delta R$  gives an indication of a change in the complex shear modulus,  $G_f'$  and  $G_f''$ , a complex relationship exists between the  $\Delta R$  values and the corresponding effects on  $G_f'$  and  $G_f''$ . A certain measured magnitude of the  $\Delta R$  alone does not determine a set absolute change in the values of  $G_f'$  and  $G_f''$ . It is our intention here to show the QCM/HCC capabilities and initial measurements of the motional resistance. Further analysis of the motional resistance values and a treatment of our method of extracting shear modulus information is presented in another reference.<sup>41</sup>

## Conclusion

The QCM/HCC provides a unique means of measuring mass changes, thermal effects, and motional resistance data in a thin film upon vapor sorption. The data shown here are collected in real-time sorption measurements monitoring equilibration steps at constant vapor activity followed by incremental vapor activity changes. From these measurements it is possible to then determine the  $\Delta_{\text{sorption}}H$  for thin films interacting with a gaseous adsorbate and the sorption isotherms for the films under study. An added feature includes the ability to monitor the motional resistance of the thin film undergoing vapor sorption. The motional resistance is related to the complex shear modulus of the film and gives an indication of the rigidity or viscoelasticity of the film.

In this study, a comparison was conducted of ethanol and water sorption among polymer films of varying thicknesses. From the results it is seen that the technique provides a powerful means of analyzing sorption enthalpies of thin films exposed to vapor sorption. Direct calorimetric analysis is possible rather than time-consuming curve fitting of temperature dependent parameters. The calorimetric data provides a view into the type of interaction of the vapor with the thin film.

## Acknowledgements

The authors would like to thank several former undergraduate researchers who helped in film preparations and experimental runs: Anna Ayropetova, Elizabeth Jacob, Rebecca Mason, and Jason Riggs.

## References

1. Cannon, L. A.; Pethrick, R. A. *Macromolecules* 1999, 32, 7617-7629.
2. Ngui, M. O.; Mallapragada, S. K. *Journal of Applied Polymer Science* 1999, 72, 1913-1920.
3. Saby-Dubreuil, A.-C.; Guerrier, B.; Allain, C.; Johannsmann, D. *Polymer* 2001, 42, 1383-1391.
4. Price, G. J.; Buley, J. M. *Progress in Organic Chemistry* 1991, 19, 265-274.
5. Bunde, R. L.; Jarvi, E. J.; Rosentreter, J. J. *Talanta* 1998, 46, 1223-1236.
6. Rodahl, M.; Hook, F.; Fredriksson, C.; Keller, C. A.; Krozer, A.; Brzezinski, P.; Voinova, M.; Kasemo, B. *Faraday Discussions* 1997, 107, 229-246.
7. Sakti, S. P.; Rösler, S.; Lucklum, R.; Hauptmann, P.; Bühling, F.; Ansorge, S. *Sensors and Actuators A* 1999, 76, 98-102.
8. Bluestein, S. D.; Chan, E. K.; Miaoulis, I. N.; Wong, P. Y. *IEEE Transactions on Components and Packaging Technology* 1999, 22, 421-425.
9. Hilic, S.; Boyer, S. A. E.; Pádua, A. A. H.; Grolier, J.-P. E. *Journal of Polymer Science: Part B: Polymer Physics* 2001, 39, 2063 - 2070.
10. Lucklum, R.; Henning, B.; Hauptmann, P.; Schierbaum, K. D.; Vaihinger, S.; Goepel, W. *Sensors and Actuators, A* 1991, A27, 705-710.
11. Matsuura, K.; Ebara, Y.; Okahata, Y. *Langmuir* 1997, 13, 814-820.
12. Schierbaum, K. D.; Gerlach, A.; Haug, M.; Goepel, W. *Sensors and Actuators A* 1992, A31, 130-137.
13. Grate, J. W.; Patrash, S. J.; Abraham, M. H.; Du, C. M. *Analytical Chemistry* 1996, 68, 913-917.
14. Grate, J. W.; Wise, B. M. *Analytical Chemistry* 2001, 73, 2239-2244.
15. Buchold, R.; Nakladal, A.; Gerlach, G.; Herold, M.; Gauglitz, G.; Sahre, K.; Eichhorn, K. J. *Thin Solid Films* 1999, 350, 178-185.
16. Smith, A. L.; Shirazi, H. M. *Journal of Thermal Analysis and Calorimetry* 2000, 59, 171-186.
17. Brodt, M.; Cook, L. S.; Lakes, R. S. *Review of Scientific Instruments* 1995, 66, 5292-5297.
18. Domack, A.; Johannsmann, D. *Journal of Applied Physics* 1996, 80, 2599-2604.
19. Vinci, R. P.; Vlassak, J. J. *Annual Review of Materials Science* 1996, 26, 431-462.
20. Tian, J. In Ph.D. Thesis; Drexel University: Philadelphia, PA, 2002.
21. Shirazi, H. M. In Ph.D. thesis; Drexel University: Philadelphia, PA, 2000, p 341.
22. Smith, A. L.; Shirazi, H. M.; Mulligan, S. R. *Biochimica et Biophysica Acta* 2002, 1594, 150-159.
23. Tian, J.; Smith, A. L. *Proceedings of the 201st Meeting of the Electrochemical Society, Philadelphia, May 12 - 17, 2002* 2002, pp 255-269.
24. Sauerbrey, G. *Z. Z. Phys.* 1959, 206-222.
25. Buttry, D. A.; Ward, M. D. *Chemical Reviews* 1992, 92, 1355-1379.
26. Lu, C.; Czanderna, A. W. *Application of Piezoelectric Quartz Crystal Microbalances*; Elsevier: Amsterdam, 1984.
27. Behling, C.; Lucklum, R.; Hauptmann, P. *Measurement Science Technology* 1998, 9, 1886-1893.
28. Hillman, A. R.; Jackson, A.; Martin, S. J. *Analytical Chemistry* 2001, 73, 540-549.

29. Lee, S.-W.; Hinsberg, W. D.; Kanazawa, K. K. *Analytical Chemistry* 2002, 74, 125-131.
30. Lucklum, R.; Hauptmann, P. *IEEE International Frequency Control Symposium and PDA Exhibition, 2001*, pp 408 - 417.
31. Martin, S. J.; Bandey, H. L.; Cernosek, R. W.; Hillman, A. R.; Brown, M. J. *Analytical Chemistry* 2000, 72, 141-149.
32. Muramatsu, H.; Kimura, K. *Analytical Chemistry* 1992, 64, 2502-2507.
33. Johannsmann, D. *Journal of Applied Physics* 2001, 89, 6356-6364.
34. Rodahl, M.; Kasemo, B. *Sensors and Actuators, B* 1996, B37, 111-116.
35. Lucklum, R.; Hauptmann, P. *Electrochimica Acta* 2000, 45, 3907-3916.
36. Smyth, C.; Kudryashov, E. D.; Buckin, V. *Colloids and Surfaces A: Physicochemical and Engineering Aspects* 2001, 183-185, 517-526.
37. Donth, E.-J. *The Glass Transition Relaxation Dynamics in Liquids and Disordered Materials*; Springer-Verlag: Berlin, 2001.
38. Sperling, L. H. In *Sound and Vibration Damping with Polymers*; Corsaro, R., D.; Sperling, L. H., Eds.; American Chemical Society: Washington DC, 1990, p 5-22.
39. Janshoff, A.; Galla, H.-J.; Steinem, C. *Angewandte Chemie Int. Ed.* 2000, 39, 4004-4032.
40. Behling, C.; Lucklum, R.; Hauptmann, P. *Sensors and Actuators A* 1997, 61, 260-266.
41. Smith, A. L. *Journal of Polymer Science Part B: Polymer Physics*, in press.
42. Miller, J. G.; Bolef, D. I. *Journal of Applied Physics* 1968, 39, 5815 - 5816.
43. Miller, J. G.; Bolef, D. I. *Journal of Applied Physics* 1968, 39, 4589 - 4593.
44. Lu, C. S.; Lewis, O. *Journal of Applied Physics* 1972, 43, 4385-4390.
45. Wadsö, I. *Chemical Society Reviews* 1997, 26, 79-86.
46. Bäckman, P.; Bastos, M.; Hallén, D.; Lönnbro, P.; Wadsö, I. *Journal of Biochemical and Biophysical Methods* 1994, 28, 85-100.
47. Wadsö, I. *Thermochimica Acta* 1995, 267, 45-59.
48. Okuzaki, H.; Kondo, T.; Kunugi, T. *Polymer* 1999, 40, 995-1000.
49. Rivin, D.; Kendrick, C. E.; Gibson, P. W.; Schneider, N. S. *Polymer* 2001, 42, 623-635.
50. Russell, S. P.; Weinkauf, D. H. *Polymer* 2001, 42, 2827-2836.
51. Zhang, C.; Cappleman, B. P.; Defibaugh-Chavez, M.; Weinkauf, D. H. *Journal of Polymer Science: Part B: Polymer Physics* 2003, 41, 2109-2118.
52. Gregory, R. B. In *Protein-Solvent Interactions*; Gregory, R. B., Ed.; Marcel Dekker, Inc.: New York, 1995, p 191-264.
53. Ferry, J. D. *Viscoelastic Properties of Polymers*; John Wiley and Sons: New York, 1980.
54. Fitzgerald, E. R.; Ferry, J. D.; Fitzgerald, R. E. *Numerical Modelling and Related Topics*, Harrogate, July 6-8, 1998 1998.
55. Aklonis, J. J.; MacKnight, W. J. *Introduction to Polymer Viscoelasticity*; John Wiley and Sons: New York, 1983.
56. Göpel, W. *Sensors and Actuators B* 1994, 18-19, 1-21.
57. Lide, D. R., Ed. *CRC Handbook of Chemistry and Physics*; CRC Press: New York, 1997.
58. Guerrier, B.; Bouchard, C.; Allain, C.; Bénard, C. *AIChE* 1998, 44, 791-798.

59. Bone, S. *Phys. Med. Biol.* 1996, 41, 1265-1275.
60. Lüscher-Mattli, M.; Rüegg, M. *Biopolymers* 1982, 21, 403-418.
61. Lucklum, R.; Behling, C.; Hauptmann, P.; Cernosek, R. W.; Martin, S. J. *Sensors and Actuators A* 1998, 66, 184-192.